Supporting Information

High CO₂ separation performance on a metal-organic framework comprised of Nano-cages lined with ultra-high density of dual-side open metal sites

Liangjun Li,[a*] Jiangxiu He,[ad] Wenli Xu,[a] Kuitong Zhang,[b] Tao Xing,[b] Zhi Li,[be] Dewen Zhen,[c*] Bo Xiong,[c] Zhixing Ge,[c] Qian Zhang,[c] Shanyu Wang,[c] Fuzhao Zhang,[a] Xing Gu,[a] Pengcheng Dai,[a] Dandan Liu,[a] Lingzhi Yang[a] and Xuebo Zhao[a*]

[a] Institute of New Energy, College of New Energy, China University of Petroleum (East China), Qingdao, 266580, P. R. China. Email: lilj@upc.edu.cn

[b] New Energy Division, Shandong Energy Group Co., LTD. Zoucheng, Jining, China

[c] New Energy Department, Research Institute of Petroleum Exploration & Development, China National Petroleum Corporation, Langfang, 065007, zdw69@petrochina.com.cn

[d] Sinopec Qingdao Petrochemical Co., LTD., Qingdao, 266580, China

[e] School of Materials Science and Engineering, Xi'an Jiaotong University,

Contents

S1 Experimental details

1. General Information

All of the starting materials including inorganic salt, organic solvents and the ligand: 1H-pyrazole-4-carboxylic acid (H_2PCA) were purchased from commercial lines and were used without further purification.

Single-crystal X-ray diffraction data were collected on a Bruker SMART APEX2 diffractor equipped with graphite-monochromatic Mo-Kα radiation. Data reductions and adsorption corrections were performed using SADABS[1] and SAINT[2] programs, respectively. The structure of MOF was solved by direct methods and was refined by difference Fourier techniques using the SHELXTL software package.[3] Hydrogen atoms on the ligand were placed in idealized positions and were refined using a riding model. Solvents molecules in the unit cell were so highly disordered that they could not be located. To solve this problem, the contribution of electron density of solvent molecules was removed using PLANTON/SQUEEZE program.[4] Due to the high porosity and flexibility of the ligand, some of atoms in MOF's framework are highly disordered. To solve this issue, some of disordered atoms were treated by restraints and were not subjected to further anisotropic refinements.

Powder X-ray diffraction was recorded on a PANalytical X'pert PRO (Holland) X-ray diffractometer with a Cu-Ka radiation source. N_2 adsorption isotherms at 77 K were conducted on an Autosorb-iQ analyser (Quantachrome, USA).

Gas adsorption isotherms and kinetic profiles for CO_2, N_2, CH_4, C_2H_4, C_2H_6, C_3H_6 and C_3H_8 at room temperatures were measured by a gravimetric adsorption analyzer equipped with a magnetic suspension balance (XEMIS, Hidden, UK). About 100 mg sample was introduced into the XEMIS for gas sorption measurements. Before gas adsorption measurements, the MOF was activated at 120℃ and high vacuum for 12 hours. The adsorption temperature was controlled with a program-controlled water bath jacket. The set pressure point was maintained by computer control throughout the course of the experiment.

The computational Grand canonical Monte Carlo (GCMC) simulations for density distributions of gas molecules on [$Cu_3(μ_3$-OH)(PCA)$_3$] were performed by using the RASPA[5] software. Nonbonded interactions between the gas molecules and MOFs' framework were calculated using the Lennard-Jones (L-J) potential. The cross-L-J parameters were determined using the Lorentz-Berthelot mixing

rules. The TraPPE forcefield was employed for gas molecules, and the GeneralMOF forcefield was used for MOFs' framework atoms.[6] The pore structural parameters including pore volumes were calculated using the Zeo^{++} software package.[7]

2. Synthesis of [Cu$_3$(μ$_3$-OH)(PCA)$_3$]:

The MOF was synthesized under a solvo-thermal condition. H$_2$PCA(0.336 g, 3.0 mmol) and Cu(NO$_3$)$_2$·3H$_2$O (0.483 g, 2.0 mmol), DMF (20 ml), EtOH (20 ml) and water (15 ml) were added into a Telfon-lined container (100 mL). After stirring at ambient conditions for 30 minutes, the Teflon-lined container was then sealed and was placed in a programed oven. The oven was heated up to 80℃ and was kept at 80℃ for 72 hours. After cooling to room temperature, deep blue single crystals with a block morphology were obtained by filtration. Large single crystals of MOF with good quality were selected for single-crystal X-ray diffraction analysis. Large scale synthesis of this MOF was conducted under the similar conditions but with 10 times of ligands, salts and solutions.
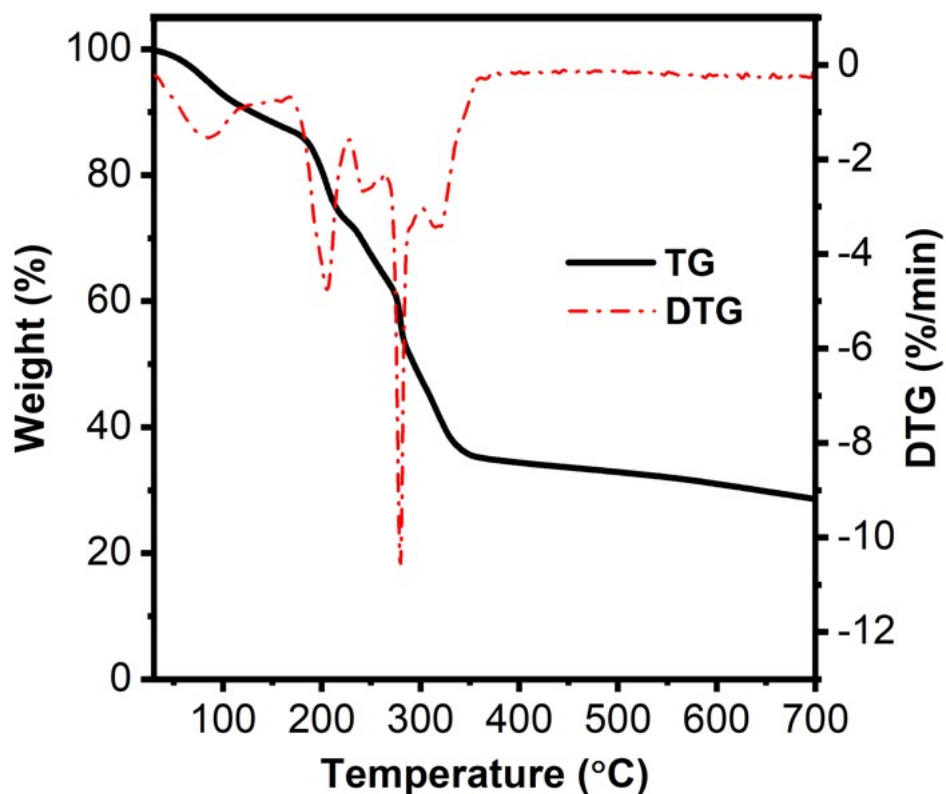
S2 TGA curve

Figure S1 TGA curve of the MOF: [Cu$_3$(μ$_3$-OH)(PCA)$_3$]

S3 Calculation details of adsorption enthalpy

The adsorption enthalpy for these gases were calculated using the Clausius-Clapeyron (equation 1)

$$\frac{d(lnP)}{d(1/T)} = \frac{Q_{st}}{R}$$

(1)

Based on the Clausius-Clapeyron , the $d(lnP)/d(1/T)$ at a certain loading can be derived from the linear fitting of lnP vs. $1/T$ (as shown in Figure S2). Then, the Q_{st} value can be calculated from the as $R* d(lnP)/d(1/T)$.
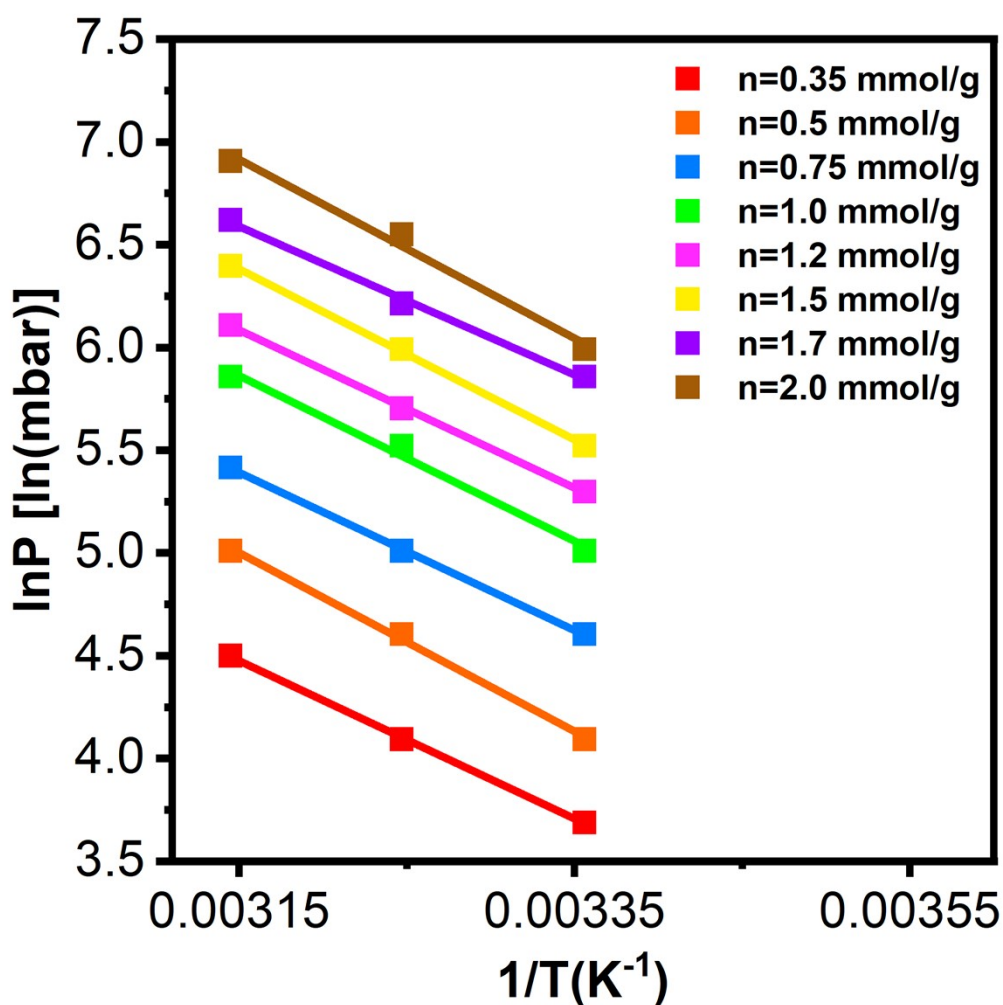

Figure S2 a) the linear fitting plot of lnP vs. 1/T

S4 Calculation details of the IAST selectivity

The thermodynamic separation selectivity of gas mixtures on $[Cu_3(\mu_3\text{-}OH)(PCA)_3]$ is calculated using the ideal adsorbed solution theory (IAST) method. Firstly, the adsorption isotherms of CO_2, CH_4, N_2 and O_2 are fitted by the dual Langmuir-Frundlich model (DSLF) using the following equation:

$$N = N_1 \times \frac{b_1 P^{1/m1}}{1 + b_1 P^{1/m1}} - N_2 \times \frac{b_2 P^{1/m2}}{1 + b_2 P^{1/m2}} \tag{1}$$

in which, P is the pressure of adsorbed phase, N_1 and N_2 are maximum loading on sites 1 and 2, b_1 and b_2 are the affinity constants of sites 1 and 2, and m_1 and m_2 are used to describe the deviation from the ideal Langmuir equation.

The fitting parameters of adsorption isotherms of CO_2, N_2 and CH_4 at 298 K by DSLF equation are listed in Table S1.

Table S1 The fitting parameters of adsorption isotherms of CO_2, CH_4, N_2 and O_2 by DSLF equation

Adsorbates	N_1	b_1	m_1	N_2	b_2	m_2
CO_2	2.98215	2.99803	1.00195	2.67542	0.35141	0.98085
N_2	0.62005	0.22586	0.91061	4.46694	0.01255	0.9382
CH_4	1.20228	0.47277	0.83244	1.12337	0.32263	1.41516

After fitting, the thermodynamic separation selectivity of O_2/N_2 and CO_2/CH_4 can be calculated using the IAST method which is depicted by following equations:

$$\pi_i^0(p_i^0) = \frac{RT}{A} \int_0^{p_i^0} q \cdot d \, lnP \tag{2}$$

$$\pi^* = \frac{\pi A}{RT} = \int_0^{p_i^0} \frac{q_i}{P} dP \tag{3}$$

$$\pi = \pi_i = \pi_j \ (i \neq j) \tag{4}$$

$$P \times y_i = P_i^0(\pi^*) \cdot x_i \tag{5}$$

$$\frac{1}{q_i} = \sum_i^n \frac{x_i}{q_i^0(P_i^0)} \tag{6}$$

$$S_{ij} = \frac{P_i^0}{P_j^0} = \frac{Py_i/x_i}{Py_j/x_j} = (\frac{x_j}{y_j})(\frac{y_i}{x_i}) \tag{7}$$

Where, A is the specific surface area of the adsorbent; π and π^* are the spreading pressure and the reduced spreading pressure, respectively; q_i is corresponding gas phase pressure of component i; P_i^0 is the pressure of component i in its standard state which is fixed by the spreading pressure of mixture according to equation 4; x_i and y_i are the mole fraction of component of i in the adsorbed

phase and bulk phase, respectively; S_{ij} is the thermodynamic separation selectivity for component i to j.

Upon numerical solution of above equations, the thermodynamic separation selectivity for CO_2/N_2, CO_2/CH_4, CH_4/N_2 at different pressures and different gas concentration can be calculated.

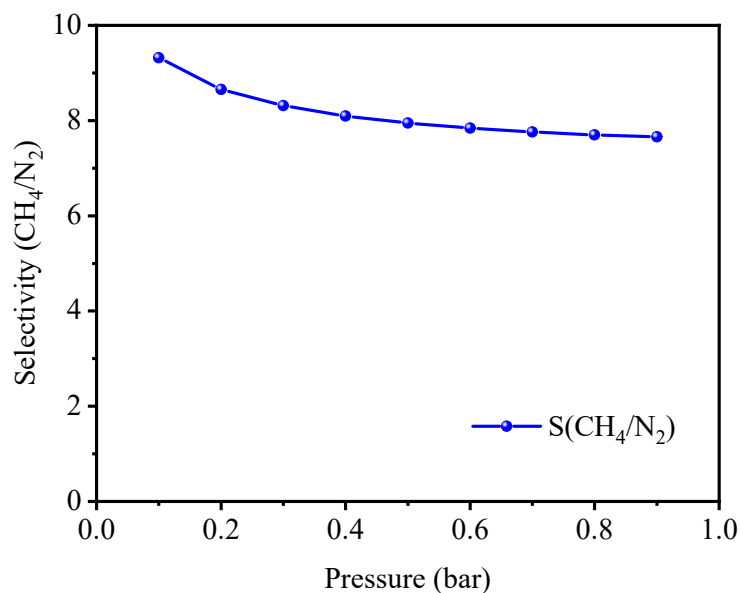For CH_4/N_2, the IAST selectivity is shown in Figure S3.

Figure S3 The equilibrium separation selectivity for equimolar CH_4/N_2 mixtures calculated from IAST method.

S5 Comparison table with literature results

Table S2 The comparison table with literature results

MOFs	$S(CO_2/N_2)$	$S(CO_2/CH_4)$	References
$[Cu_3(\mu_3\text{-}OH)(PCA)_3]$	70 (50/50) @ 298 K	15.9 (50/50) @ 298 K	This work
HKUST-1	21 (50/50) @ 298 K	5.5 (50/50) @303 K	[8-10]
Mg-MOF-74	182(85/15) @296 K	105.1(50/50) @296 K	[11, 12]
NOTT-101	12.4 (50/50) @293 K	4.6 (50/50) @293 K	[13]
PCN-88	15.2 (85/15) @296 K	5.8 (50/50) @296 K	[14]
ZIF-78	41.4 (85/15) @296 K	10.4 (50/50) @296 K	[14]
USTA-16	315 (85/15) @296 K	29.8 (50/50) @296 K	[11]
SIFSIX-2-Cu	13.7 (90/10) @298 K	5.3 (50/50) @298 K	[15]

| SIFSIX-2-Cu-i | 140 (90/10) @298 K | 33 (50/50) @298 K | 15, 16 |
| SIFSIX-3-Zn | 1700 (90/10) @298 K | 231 (50/50) @298 K | 15, 16 |

References

1. G. M. Sheldrick, University of Göttingen, Germany, 2004.

2. Bruker, Bruker AXS Inc., Madison, Wisconsin, USA., 2007.

3. G. Sheldrick, *Acta Crystallogr. A*, 2008, **64**, 112-122.

4. A. Spek, *J. Appl. Crystallogr.*, 2003, **36**, 7-13.

5. D. Dubbeldam, S. Calero, D. E. Ellis and R. Q. Snurr, *Mol. Simulat.*, 2016, **42**, 81-101.

6. Z. Li, F. Liao, F. Jiang, B. Liu, S. Ban, G. Chen, C. Sun, P. Xiao and Y. Sun, *Fluid Phase Equilibr.*, 2016, **427**, 259-267.

7. T. F. Willems, C. H. Rycroft, M. Kazi, J. C. Meza and M. Haranczyk, *Micropor. Mesopor. Mat.*, 2012, **149**, 134-141.

8. L. Hamon, E. Jolimaître and G. D. Pirngruber, *Ind. Eng. Chem. Res.*, 2010, **49**, 7497-7503.

9. S. Cavenati, C. A. Grande, A. E. Rodrigues, C. Kiener and U. Müller, *Ind. Eng. Chem. Res.*, 2008, **47**, 6333-6335.

10. B. Liu and B. Smit, *Langmuir*, 2009, **25**, 5918-5926.

11. S. Xiang, Y. He, Z. Zhang, H. Wu, W. Zhou, R. Krishna and B. Chen, *Nat. Commun.*, 2012, **3**.

12. S. R. Caskey, A. G. Wong-Foy and A. J. Matzger, *J. Am. Chem. Soc.*, 2008, **130**, 10870-10871.

13. C. Wang, L. Li, S. Tang and X. Zhao, *ACS Appl. Mater. Interfaces*, 2014, **6**, 16932-16940.

14. J.-R. Li, J. Yu, W. Lu, L.-B. Sun, J. Sculley, P. B. Balbuena and H.-C. Zhou, *Nat. Commun.*, 2013, **4**, 1538.

15. P. Nugent, Y. Belmabkhout, S. D. Burd, A. J. Cairns, R. Luebke, K. Forrest, T. Pham, S. Ma, B. Space, L. Wojtas, M. Eddaoudi and M. J. Zaworotko, *Nature*, 2013, **495**, 80-84.

16. Y. Belmabkhout, V. Guillerm and M. Eddaoudi, *Chem. Eng. J.*, 2016, **296**, 386-397.